Non-Linear Model Predictive Control for Modular Multilevel Converters

Saad Hamayoon[1], Morten Hovd[1] and Jon Are Suul[1,2]

[1]Department of Engineering Cybernetics, Norwegian University of Science and Technology, Trondheim, Norway
[2]SINTEF Energy Research, Trondheim, Norway
email:saad.hamayoon@ntnu.no

Abstract—In this paper, non-linear model predictive control (NMPC) without an explicit modulator is applied to modular multilevel converters (MMCs) in the abc reference frame. NMPC can easily be extended for longer prediction horizons as opposed to finite control set model predictive control (FCS-MPC). However, NMPC applied to power converters in previous studies uses a modulator, which limits the transient response compared to FCS-MPC. Therefore, to avoid the modulator, two strategies are presented. In the first strategy, the continuous solution (number of inserted submodules per arm) obtained from NMPC is simply rounded off to the nearest integer for both the arms of each phase. In the second strategy, the optimal solution obtained from the NMPC is further evaluated by rounding it up and down for both arms. This requires four simulations per time step, independently from the number of SMs per arm. The evaluation of the four cases is conducted only for the initial time step within the prediction horizon. Then the solution that minimizes a pre-defined cost function is applied to MMC. The second strategy offers the fastest response and provides similar dynamic performance as indirect FCS-MPC, while both strategies offer similar steady-sate performance. Simulations are performed to validate the performance of the proposed methods compared to the FCS-MPC.

Index Terms—NMPC, differential current, model predictive control, modular multilevel converter (MMC), capacitor voltage balancing

I. INTRODUCTION

Modular multilevel converters (MMCs) have received significant attention in recent years [1], [2]. This is mainly due to the attractive properties resulting from the series connection of submodules (SMs), which allows for achieving high output voltage. Indeed, the modularity of MMCs allows for designing systems with a high number of voltage levels and limited filter requirements due to the low harmonic component in the output voltage. These features make MMCs very attractive for high voltage direct current (HVDC) transmission systems [2].

The multi-input multi-output (MIMO) nature of MMCs and the presence of internal dynamics are imposing challenges for the control system design [2]. Therefore, many control techniques have been investigated in literature for MMCs [3]–[5]. Among these, model predictive control is an effective method to easily handle constraints while dealing with the non-linearity and MIMO nature of the MMCs.

Usually, finite control set model predictive control (FCS-MPC) is used for power converters [6]. FCS-MPC takes advantage of the discrete nature of the power converters.

Therefore, in FCS-MPC, all possible switching combinations of the power converters are used to evaluate a predefined cost function. The switching combination that minimizes this cost function is then applied to the power converter in the next sampling instant. However, one problem with this approach is that when the number of switching combinations is large, long prediction horizons cannot be used due to high computational complexity. Therefore, a prediction horizon of just one time step is typically used for FCS-MPC if a high number of switching combinations have to be considered. MMCs used in HVDC application typically have very high number of SMs/arm which leads to a high number of switching combinations. Therefore, direct FCS-MPC is not feasible for this application.

Considerable work has been done in order to reduce the computational complexity of FCS-MPC to enable its practical use [7]–[11] for MMCs. All of these approaches are based on indirect FCS-MPC in which optimization is performed over voltage levels instead of switching combinations. Furthermore, the conventional or a modified sorting algorithms are used to perform the capacitor voltage balancing. In order to further reduce the computational complexity, these methods try to reduce the number of control options to be evaluated at each sampling instant by only considering the neighboring voltage levels with respect to previous sampling instant. This considerably reduces the computational complexity when compared to direct or full indirect FCS-MPC but the dynamic response of the converter becomes slow. Another approach based on indirect FCS-MPC reduced the computational complexity by evenly distributing the SMs into M groups with each containing X SMs resulting in a computational burden of $2X + M + 3$ [12]. However, no specific criterion is provided on how to group the SMs. Different from indirect FCS-MPC, a dual-stage MPC approach has been presented in [13]. This method results in a very good dynamic performance, however, its computational complexity is much higher when compared to indirect FCS-MPC approaches.

Recently, some other variants of indirect FCS-MPC methods have been presented to address the issue of slow dynamic performance, while keeping the computational complexity low [14]–[17]. In [14], the steady-state and transient state are handled individually. In steady-state, the number of options to be evaluated are the same as in most indirect FCS-MPC strategies, however, they are increased in the transient state

which allows for high dynamic performance. In [15], the improvement in dynamic performance is achieved by allowing the number of inserted SM to change by more than one only in the initial step within the prediction horizon. This method does not have to detect when a transient state is occurring. Both of these methods achieve high dynamic performance with low computational complexity for MMCs as compared to other FCS-MPC strategies. However, when dealing with MMCs having hundreds of SMs per arm, these methods would have to consider more number of options to ensure proper operation, thus increasing the computational complexity. In [16], backstepping is combined with reduced indirect FCS-MPC and the work in [17] applies a bisection algorithm in the first stage and reduced indirect FCS-MPC in the second stage. These methods simplify the first stage by assuming that the total number of inserted SMs are always equal to N (total number of SMs/arm). Therefore, when the number of SMs is higher, then these methods would need to consider more number of options in the second stage which will result in increased computational burden.

In this work, continuous set non-linear model predictive control (NMPC) will be applied to MMC. Due to the progress made over the last decade, the computational complexity of NMPC is not anymore a significant challenge for most practical applications [18]. However, in power electronics where the sampling times are usually very small further work is required. The benefit of NMPC will be that it can easily be extended for longer prediction horizons and thus offer better performance. The earlier works based on NMPC [19]–[21] use PWM modulators. Due to the presence of these modulators, the dynamic response of NMPC is worse as compared to FCS-MPC [22], [23]. Similarly to the indirect FCS-MPC, the NMPC proposed in this paper does not require a separate modulator. Therefore, instead of PWM modulators, only the conventional sorting algorithm is used, which directly provides the switching sequence to MMC. The absence of modulator would result in slightly reduced steady-state performance. Solutions exist to address this issue without the inclusion of explicit modulator [22]. However, this is not the focus of this work, so interested readers are suggested to read [22] and references therein.

The optimal solution (number of inserted SMs) obtained from NMPC will be continuous. To avoid the modulator, this needs to be converted to a discrete value as the number of inserted SMs can only be discrete. Therefore, two strategies are presented to deal with this. In the first strategy, the solution obtained is simply rounded off to the nearest integer for both the arms of each phase. In the second strategy, the optimal solution obtained is tested by rounding it down and rounding it up for both upper and lower arms. This would require four simulations per time step, independently of the number of SMs/arm. It is noted here that the rounding up/down is done only for the initial time step in the prediction horizon. The proposed second strategy offers similar steady-state and dynamic performance as compared to indirect FCS-MPC. However, the first strategy suffers from sluggish dynamic
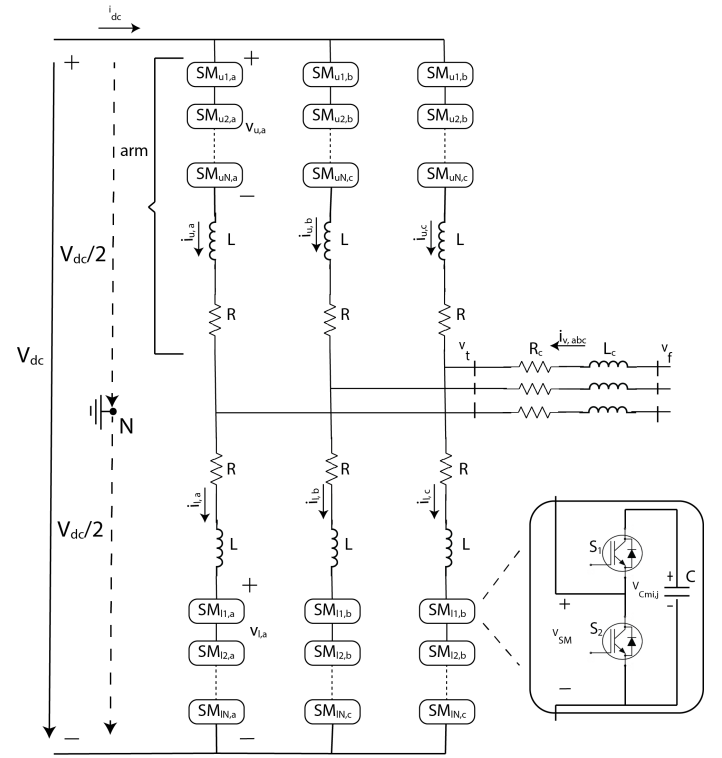

Fig. 1. Circuit Diagram of MMC

response.

The rest of the paper is organized as follows. The MMC model and operation is presented in Section II. In Section III, the proposed method is explained. Finally, the performance of the proposed method is validated through simulations in Section IV.

II. MODEL OF THE MMC

The modeling presented in this section is based on [15]. Figure 1 depicts the three-phase MMC system where each phase of the MMC consists of two arms *i.e.* an upper arm and a lower arm denoted by u and l respectively. Each arm consist of N half-bridge submodules (SM), an inductor and a resistor. The arm inductor is used to limit the harmonics and fault currents and the arm resistor is used for modeling the losses of the MMC. Depending on the switching states of S_1 and S_2, each SM can provide two voltage levels *i.e.* 0 or $v_{Cm_{i,j}}$ where the index $m = u, l$ identifies the upper or lower arm, $i = 1, 2, \ldots, N$ identifies the individual sub-module within the arm, and $j = a, b, c$ identifies the phase.

Based on Kirchoff's voltage law, the mathematical model of the MMC shown in Fig. 1 can be expressed as:

$$\frac{V_{dc}}{2} - v_{u,j} - R i_{u,j} - L \frac{di_{v,j}}{dt} + R_c i_{v,j} + L_c \frac{di_{v,j}}{dt} - v_f = 0 \quad (1)$$

$$\frac{V_{dc}}{2} - v_{l,j} - R i_{l,j} - L \frac{di_{l,j}}{dt} - R_c i_{v,j} - L_c \frac{di_{v,j}}{dt} + v_f = 0 \quad (2)$$

where $v_{u,j}$ and $v_{l,j}$ represent the upper and lower arm voltages of phase j, $i_{u,j}$ and $i_{l,j}$ represent the upper and lower arm

currents of phase j, $i_{v,j}$ is the ac-side current, V_{dc} is the dc-side voltage, v_f is the grid side voltage, R is the arm resistance, L is the arm inductance, R_c and L_c are the grid side converter resistance and inductance, respectively.

The ac-side current and differential current are given by:

$$i_{v,j} = i_{l,j} - i_{u,j} \tag{3}$$

$$i_{diff,j} = \frac{i_{u,j} + i_{l,j}}{2} \tag{4}$$

where $i_{diff,j}$ is the differential current.

By subtracting (1) and (2) and using (3) the dynamic equation for, ac-side current is obtained as:

$$\frac{di_{v,j}}{dt} = \frac{-(R + 2R_c)}{L + 2L_c}i_{v,j} + \frac{v_{u,j} - v_{l,j}}{L + 2L_c} + \frac{2v_{f,j}}{L + 2L_c} \tag{5}$$

Similarly, by adding (1) and (2) and using (4), the dynamic equation for the differential current is obtained as:

$$\frac{di_{diff,j}}{dt} = \frac{-R}{L}i_{diff,j} - \frac{1}{2L}(v_{u,j} + v_{l,j}) + \frac{1}{2L}V_{dc} \tag{6}$$

The arm voltages $v_{u,j}$ and $v_{l,j}$ depend on the number of SM inserted in that arm. Assuming that SM capacitor voltages are well balanced at their reference values, the arm voltages can be expressed as:

$$v_{u,j} \approx \frac{n_{u,j}}{N}v_{u,j}^{\Sigma} \tag{7}$$

$$v_{l,j} \approx \frac{n_{l,j}}{N}v_{l,j}^{\Sigma} \tag{8}$$

where $n_{u,j}$ and $n_{l,j}$ are the number of SMs to be inserted in upper and lower arm respectively and $v_{u,j}^{\Sigma}$ and $v_{l,j}^{\Sigma}$ are the summation of all capacitor voltages in the upper and lower arm respectively.

The dynamics of the total arm capacitor voltages can be expressed as:

$$\frac{dv_{m,j}^{\Sigma}}{dt} = \frac{i_{m,j}}{C_{m,j}^{e}} = \frac{n_{m,j}i_{m,j}}{C} \tag{9}$$

where $C_{m,j}^{e}$ is the equivalent arm capacitance of inserted SMs in arm m. Using (3) and (4) into (9) the following dynamic equations for total arm capacitor voltages of both arms can be derived:

$$\frac{dv_{u,j}^{\Sigma}}{dt} = -\frac{n_{u,j}i_{v,j}}{2C} + \frac{n_{u,j}i_{diff,j}}{C} \tag{10a}$$

$$\frac{dv_{l,j}^{\Sigma}}{dt} = \frac{n_{l,j}i_{v,j}}{2C} + \frac{n_{l,j}i_{diff,j}}{C} \tag{10b}$$

Using the definition of $v_{u,j}$ and $v_{l,j}$ from (7) and (8) into (5) and (6), the dynamic equations for ac-side current and differential current are modified as:

$$\frac{di_{v,j}}{dt} = \frac{-(R + 2R_c)}{L + 2L_c}i_{v,j} + \frac{n_{u,j}v_{u,j}^{\Sigma} - n_{l,j}v_{l,j}^{\Sigma}}{N(L + 2L_c)} + \frac{2v_{f,j}}{L + 2L_c} \tag{11a}$$

$$\frac{di_{diff,j}}{dt} = \frac{-R}{L}i_{diff,j} - \frac{(n_{u,j}v_{u,j}^{\Sigma} + n_{l,j}v_{l,j}^{\Sigma})}{2NL} + \frac{V_{dc}}{2L} \tag{11b}$$

Using (10) and (11) the state space equation of the MMC is shown by (12)

$$\dot{x}(t) = Ax(t) + \sum_{i=1}^{2}(B_{ix}u_i) + d(t) \tag{12}$$

where $x = [i_{v,j}, i_{diff,j}, v_{u,j}^{\Sigma}, v_{l,j}^{\Sigma}]^T$ is the state vector, $u = [u_1 u_2]^T = [n_{u,j} n_{l,j}]^T$ is the input vector, $d(t)$ is the disturbance and

$$A = \begin{bmatrix} -\dfrac{(R + 2R_c)}{L + 2L_c} & 0 & 0 & 0 \\ 0 & -\dfrac{T_s R}{L} & 0 & 0 \\ 0 & 0 & 0 & 0 \\ 0 & 0 & 0 & 0 \end{bmatrix}$$

$$B_{ix} = \begin{bmatrix} B_1 x(t) & B_2 x(t) \end{bmatrix}$$

$$B_1 = \begin{bmatrix} 0 & 0 & \dfrac{1}{(L + 2L_c)N} & 0 \\ 0 & 0 & \dfrac{-1}{2NL} & 0 \\ \dfrac{-1}{2C} & \dfrac{1}{C} & 0 & 0 \\ 0 & 0 & 0 & 0 \end{bmatrix}$$

$$B_2 = \begin{bmatrix} 0 & 0 & 0 & \dfrac{-1}{(L + 2L_c)N} \\ 0 & 0 & 0 & \dfrac{-1}{2NL} \\ 0 & 0 & 0 & 0 \\ \dfrac{1}{2C} & \dfrac{1}{C} & 0 & 0 \end{bmatrix}$$

$$d(t) = \begin{bmatrix} \dfrac{2v_{f,j}(t)}{(L + 2L_c)} \\ \dfrac{V_{dc}(t)}{2L} \\ 0 \\ 0 \end{bmatrix}$$

Equation (12) shows that the MMC is a bilinear system with multiple inputs and outputs.

III. PROBLEM FORMULATION FOR PROPOSED METHOD

The control goals of the MMC are to regulate the ac-current to its reference, minimize the ac-components in the differential current and to regulate the arm summation voltages at their references. The reference for ac-side current, differential current and summation voltages are calculated as in [7] and a conventional sorting algorithm is used for SM capacitor voltage balancing as in [7]. The definition of the references is repeated here for completeness. The power equations in the dq frame are used to obtain the reference value for the ac-side current as follows:

$$i_d = \frac{2}{3}\frac{Pv_d + Qv_q}{v_d^2 + v_q^2} \tag{13a}$$

$$i_q = \frac{2}{3}\frac{Pv_q - Qv_d}{v_d^2 + v_q^2} \tag{13b}$$

Then the reference current can be obtained in the abc frame by dq to abc transformation. The differential current reference

as a first step is based on the assumption of equal input and output power and is given as:

$$I_{dc,ref} = -\frac{P}{V_{dc,ref}}, I_{diff,ref} = \frac{I_{dc,ref}}{3} \qquad (14)$$

With the above control goals and references, the stage cost function is selected as:

$$J_j = \lambda_1(i_{v,j,ref} - i_{v,j})^2 + \lambda_2(i_{diff,ref} - i_{diff,j})^2 \quad (15)$$

The λ's are the weighting factors for setting the relative importance between the control objectives. The first term in the cost function is used to keep the ac-side current at its reference, the second term is for minimizing the ac-components in the differential currents. The other two objectives *i.e.* keeping the average value of summation of capacitor voltages of each arm at their reference values are met by adjusting the reference of the differential current either in the outer loop or by having its equivalent within MPC implementation [24]. This is required because of the assumption of equal input and output power, when determining the reference for differential current. Therefore, in the outer loop a fundamental frequency component is introduced in the differential current reference to regulate arm voltage difference to zero and a dc-component is introduced if the sum of summation voltages is not regulated to $2V_{dc}$

Now, the model in (12) can be discretized by any integration method. In this work, Runge-Kutta 4 method is used for discretization. The constraints on the inputs of the system are linear and given as:

$$0 \le u_1 \le N$$
$$0 \le u_2 \le N$$
$$u_1 + u_2 \le N + 2$$
$$u_1 + u_2 \ge N - 2$$

where N is the total number of SMs in each arm of the MMC. The first two constraints are physical constraints *i.e.* the number of inserted modules per arm cannot be negative and cannot be more than the total number of SMs in that arm. The other two constraints ensure that the total number of switched on modules are not too far from N because in normal operation the total number of voltage levels should be near N. It is noted here, that the reference of summation voltages is fixed to V_{dc} for this work. If the reference is not fixed then the constraints three and four need to be modified. Moreover, in addition to the constraints defined above, linear constraints can also be imposed on state variables.

With the above problem, NMPC is applied using CasADi in MATLAB to get the continuous optimal solution. In order to avoid the modulator, two strategies are presented to deal with the continuous solution of the NMPC. In the first strategy (Case I), this solution is simply rounded off to the nearest integer and is sent to the conventional sorting algorithm. In the second strategy (Case II), the solution obtained from NMPC for both arms is rounded up and rounded down. This would require only four simulations per time step. It is noted here that
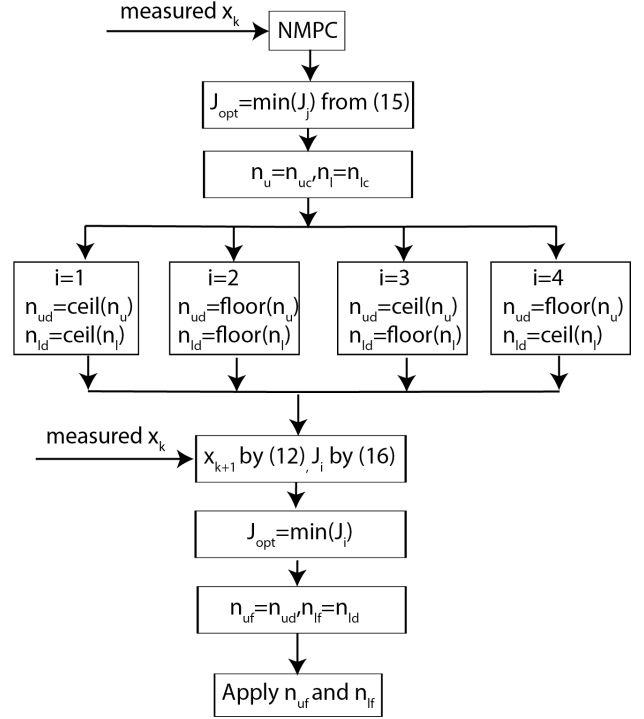

Fig. 2. Block diagram for Proposed Method

the rounding operations are only performed for the solution in the first step of the prediction horizon.

Recently, a new cost function was proposed in [17], which eliminates the need for having any kind of additional control over the differential current reference in order to regulate the average summation voltages in both arms. In the second stage of the proposed method, the four options are evaluated by this new cost function which is reproduced below:

$$J_{j,new} = \lambda_1(i_{v,j,ref} - i_{v,j})^2 + \lambda_2(i_{diff,ref} - i_{diff,j})^2$$
$$+ \lambda_3(2v_{dc,ref} - v_{u,j,avg}^\Sigma - v_{l,j,avg}^\Sigma)(i_{diff,ref} - i_{diff,j})$$
$$+ \lambda_4(v_{u,j,avg}^\Sigma - v_{l,j,avg}^\Sigma)\Delta W \quad (16)$$

where ΔW is the instantaneous energy difference between the lower and upper arm. The third term introduced above ensures the regulation of total leg voltage at $2V_{dc}$ and the fourth term ensures that the voltage difference between the arms is regulated to 0. The third term would only act if the sum of average summation voltages of both arms is not equal to $2V_{dc}$ and the fourth term would only act when their difference is not 0. The detailed explanation of the above cost function can be found in [17].

The cost function (16) is not used in the NMPC stage because optimizers perform more efficiently with quadratic cost function. The flowchart for Case II is shown in fig. 2 where n_{uc}, n_{lc} are the continuous solution from NMPC and n_{ud}, n_{ld} are the discrete insertion indices. It is noted here, that in Case I, an outer loop or some additional control over differential current reference is required in order to regulate the summation voltages. In this work, the method proposed in [24]
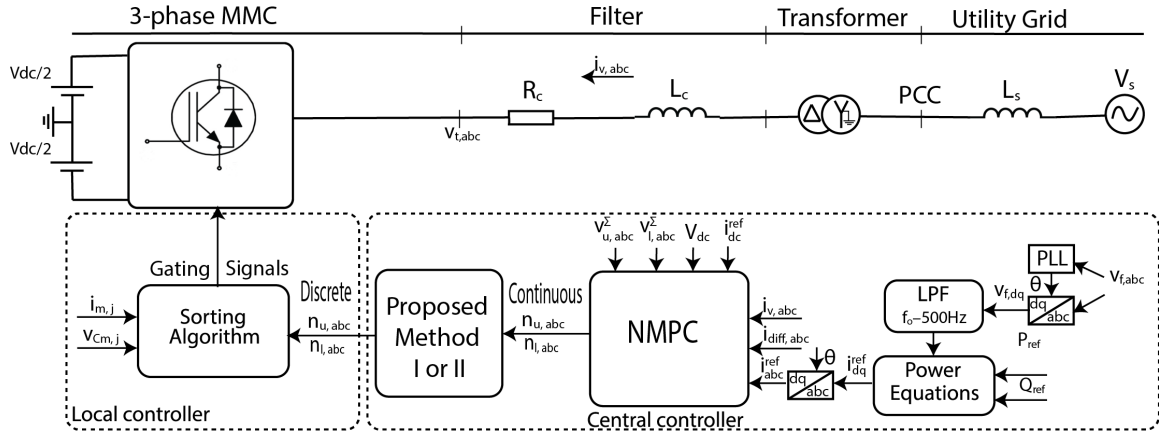
Fig. 3. Control Block Diagram of MMC

is used where the equivalent of outer loop is implemented with in MPC framework. However, this method results in higher ripples in the differential current and these ripples don't vanish even when the summation voltages are balanced.

Case I can be summarized as:

1) Continuous optimal insertion index based on the minimization of cost function (15) is obtained by NMPC
2) Round off the solution to nearest integer from step 1
3) Perform capacitor voltage balancing task based on the conventional sorting algorithm and rounded off solution from 2

Case II can be summarized as:

1) Continuous optimal insertion index based on the minimization of cost function (15) is obtained by NMPC
2) Round up and down the solution from 1
3) Select the insertion index from 2 that minimizes the cost function (16)
4) Perform capacitor voltage balancing task based on the conventional sorting algorithm and optimal insertion index from 3

IV. SIMULATION RESULTS

The block diagram for calculation of insertion index through the proposed methodology is shown in Fig. 3. The synchronization of the system with grid is achieved by using a dq-frame phase locked loop (PLL). The PLL is working to align the d-axis to the grid voltage vector in steady state. All the references and measurements are sent to the NMPC controller which outputs the continuous insertion indices. These insertion indices are then converted to discrete values using either Case I or II. Once the discrete insertion indices are obtained then they are sent to the conventional sorting algorithm which determines the gating signals for the MMC.

A. Time Domain Results

The simulation results are provided for a prediction horizon of two. The scenario used for simulation is such that, at t=0s

the reference values of active and reactive power are set to 25 MW and 0 MVar , respectively and at t = 0.15s a real power reversal command is applied by changing active power set point to −25 MW. Table I shows parameters used for simulation.

TABLE I
SIMULATION PARAMETERS

Parameter	Value
MMC nominal power (base power)	50 MVA
AC system nominal voltage (base voltage)	138 kV
Short circuit ratio at PCC	5
AC source inductance (Ls)	150 mH
Nominal frequency	60 Hz
Arm inductance (L)	7 mH
Arm resistance (R)	1Ω
Submodule capacitance (C)	14000μF
Transformer voltage rating (T)	138 kV / 30 kV
Transformer power rating	55 MVA
Transformer inductance	0.05 pu
Transformer resistance	0.01 pu
Grid side converter inductance (Lc)	5 mH
Grid side converter resistance (Rc)	0.03Ω
DC side reference voltage	60 kV
Number of SMs per arm (N)	20
Sampling time (Ts)	100μs

Figure 4 shows the dynamic response comparison of the two cases discussed in previous section and indirect FCS-MPC which considers all the possible voltage levels. Here I_{op} is for Case II, I_{rf} if for Case I and I_{in} is for indirect FCS-MPC. It can be clearly seen that Case II offers similar dynamic response as full indirect FCS-MPC. Therefore, we can conclude that the Case II is better than Case I.

Figure 5 shows the performance of all the state variables being controlled by the NMPC using Case II under active power reversal command. A longer simulation time was used to depict regulation of summation voltages. It can be seen that all the state variables and power are regulated on their references quite accurately. It can also be observed that after the transient, the differential current has both a fundamental
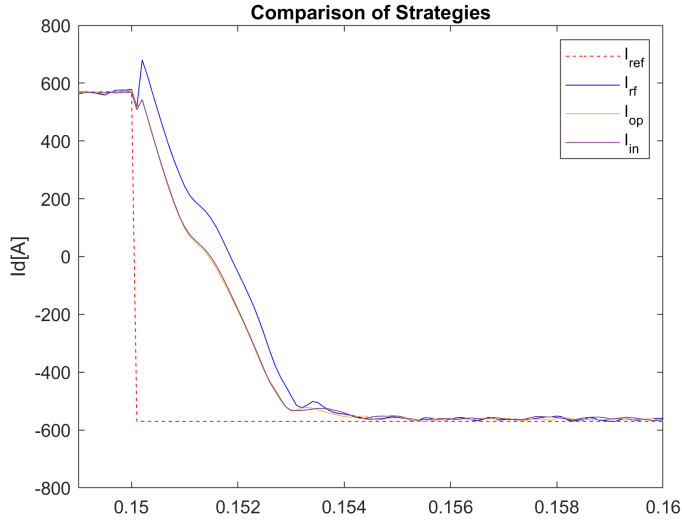
Fig. 4. Comparison of Results for d-axis component of ac-side current (Transient State): I_{rf} simple rounded off, I_{op} both rounded up and down, I_{in} Indirect FCS-MPC

frequency component and a small dc component, until the summation voltage is regulated at its reference. This change in differential current is as a result of the cost function (16).

Fig. 5. NMPC 2nd Strategy (Case II): (a) real power, (b) phase-a current, (c) phase-a differential current, (d) summation of the capacitor voltages in the lower arm of phase a

In Fig. 6, the results of Case I are shown. As highlighted earlier, it can be seen that the differential current is continuously adjusted in order to regulate the summation voltages. However, still the summation voltages are not well regulated as compared to Case II where a different cost function is used in the second stage. This shows that the equivalent of outer

loop within MPC implementation is not accurate. In case of an explicit outer loop the summation voltages are well regulated and the differential current also settles on its fixed reference once the summation voltages are balanced. However, the outer loop has its own drawbacks *i.e.* tuning of PI controllers and having slow dynamics.
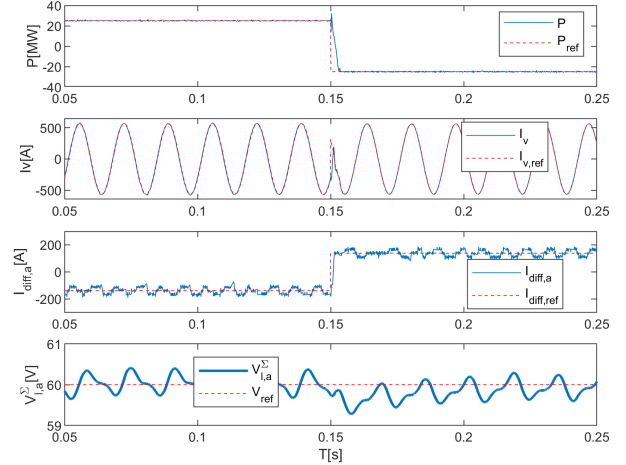

Fig. 6. NMPC 1st Strategy (Case I): (a) real power, (b) phase-a current, (c) phase-a differential current, (d) summation of the capacitor voltages in the lower arm of phase a
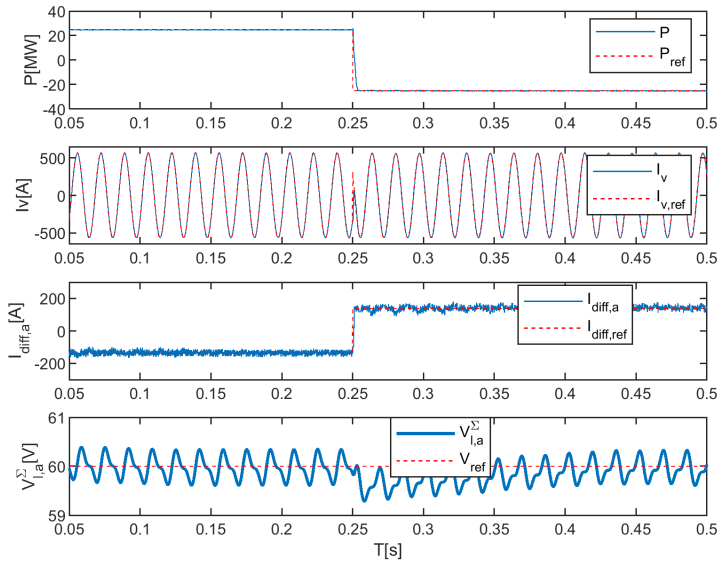
B. Computational Requirements Discussion

The time taken by full indirect FCS-MPC and NMPC for one time step for 20SMs/arm and a prediction horizon $p = 2$ are on average 0.9321 and 0.5401 seconds respectively. The simulation was made using MATLAB R2019b on Intel® Core i7, 3.20 GHz, with 16 GB RAM. It can be observed that the time taken by FCS-MPC is almost twice as compared to NMPC in this scenario. Therefore, for longer prediction horizons, NMPC should be the automatic choice. However, for $p = 1$ full indirect FCS-MPC ($0.0185s$) is faster as compared to NMPC ($0.4997s$). Therefore, due to the bilinear model and short sampling time, the computational complexity of NMPC for MMC is high thus hindering its real time application. However, it is expected that with ongoing research this computational complexity will be reduced in near future. It is noted here that the time taken by both methods are expected to be much shorter with efficient implementation on a dedicated real time platform (without much of the overhead of the operating system on a general purpose computer).

V. CONCLUSION

In this work, an NMPC strategy without modulator is proposed for MMC. Two methods were presented to deal with the continuous solution of NMPC. It was shown that the method which considers both rounded up and rounded down control options offers better dynamic performance. The NMPC problem was formulated and solved using CasADi in MATLAB with a quadratic cost function per phase and

linear constraints. The conventional sorting algorithm was used to perform the voltage balancing task. To avoid any sort of additional control on differential current reference, a different cost function was used for Case II in the second stage that ensured the regulation of summation voltages at their reference on average. Simulations demonstrate that the proposed method gives similar performance as full indirect FCS-MPC. Moreover, as compared to indirect FCS-MPC techniques the proposed method can easily be extended for longer prediction horizons.

REFERENCES

[1] K. Sharifabadi, L. Harnefors, H.-P. Nee, S. Norrga, and R. Teodorescu, *Design, Control and Application of Modular Multilevel Converters for HVDC Transmission Systems.* United States: Wiley-IEEE press, 2016.

[2] T. Geyer, Model Predictive Control of High Power Converters and Industrial Drives, Hoboken, NJ, USA:Wiley, 2016.

[3] A. Dekka, B. Wu, R. L. Fuentes, M. Perez and N. R. Zargari, "Evolution of Topologies, Modeling, Control Schemes, and Applications of Modular Multilevel Converters," *IEEE Journal of Emerging and Selected Topics in Power Electronics,* vol. 5, no. 4, pp. 1631-1656, Dec 2017

[4] A. Antonio-Ferreira, C. Collados-Rodriguez and O. Gomis-Bellmunt, "Modulation techniques applied to medium voltage modular multilevel converters for renewable energy integration: A review", *Electric Power Systems Research,* vol. 155, no. 7, pp. 21-39, Feb 2018

[5] A. Dekka, B. Wu, V. Yaramasu, R. L. Fuentes and N. R. Zargari, "Model Predictive Control of High-Power Modular Multilevel Converters—An Overview," *IEEE Journal of Emerging and Selected Topics in Power Electronics,* vol. 7, no. 1, pp. 168-183, March 2019

[6] S. Vazquez, J. Rodriguez, M. Rivera, L. G. Franquelo and M. Norambuena, "Model Predictive Control for Power Converters and Drives: Advances and Trends," *IEEE Transactions on Industrial Electronics,* vol. 64, no. 2, pp. 935-947, Feb. 2017

[7] M. Vatani, B. Bahrani, M. Saeedifard and M. Hovd, "Indirect Finite Control Set Model Predictive Control of Modular Multilevel Converters," *IEEE Transactions on Smart Grid,* vol. 6, no. 3, pp. 1520-1529, May 2015

[8] Z. Gong, P. Dai, X. Yuan, X. Wu and G. Guo, "Design and Experimental Evaluation of Fast Model Predictive Control for Modular Multilevel Converters," *IEEE Transactions on Industrial Electronics,* vol. 63, no. 6, pp. 3845-3856, June 2016

[9] B. Gutierrez and S. Kwak, "Modular Multilevel Converters (MMCs) Controlled by Model Predictive Control With Reduced Calculation Burden," *IEEE Transactions on Power Electronics,* vol. 33, no. 11, pp. 9176-9187, Nov. 2018

[10] M. H. Nguyen and S. Kwak, "Simplified Indirect Model Predictive Control Method for a Modular Multilevel Converter," *IEEE Access,* vol. 6, pp. 62405-62418, 2018

[11] J. Huang et al., "Priority Sorting Approach for Modular Multilevel Converter Based on Simplified Model Predictive Control," *IEEE Transactions on Industrial Electronics,* vol. 65, no. 6, pp. 4819-4830, June 2018

[12] P. Liu, Y. Wang, W. Cong and W. Lei, "Grouping-Sorting-Optimized Model Predictive Control for Modular Multilevel Converter With Reduced Computational Load," *IEEE Transactions on Power Electronics,* vol. 31, no. 3, pp. 1896-1907, March 2016

[13] A. Dekka, B. Wu, V. Yaramasu and N. R. Zargari, "Dual-Stage Model Predictive Control With Improved Harmonic Performance for Modular Multilevel Converter," *IEEE Transactions on Industrial Electronics,* vol. 63, no. 10, pp. 6010-6019, Oct. 2016

[14] Nguyen, M.H.; Kwak, S. "Improved Indirect Model Predictive Control for Enhancing Dynamic Performance of Modular Multilevel Converter." *Electronics* 9(9), 1405, 2020.

[15] S. Hamayoon, M. Hovd, J. A. Suul and M. Vatani, "Modified Reduced Indirect Finite Control Set Model Predictive Control of Modular Multilevel Converters," *IEEE COMPEL 2020*, Aalborg, Denmark, pp. 1-6,

[16] S. Hamayoon, M. Hovd and J. A. Suul, "Combination of Backstepping and Reduced Indirect FCS-MPC for Modular Multilevel Converters," *IECON 2021 – 47th Annual Conference of the IEEE Industrial Electronics Society,* 2021, pp. 1-6

[17] S. Hamayoon, M. Hovd and J. A. Suul, "Bisection Algorithm based Indirect Finite Control Set Model Predictive Control for Modular Multilevel Converters," *2021 IEEE 22nd Workshop on Control and Modelling of Power Electronics (COMPEL),* 2021, pp. 1-6

[18] S. Lucia, A. Tatulea-Codrean, C. Schoppmeyer and S. Engell, "Rapid development of modular and sustainable nonlinear model predictive control solutions", *Control Eng. Practice,* vol. 60, pp. 51-62, 2017.

[19] G. Darivianakis, T. Geyer and W. van der Merwe, "Model predictive current control of modular multilevel converters," *2014 IEEE Energy Conversion Congress and Exposition (ECCE),* 2014, pp. 5016-5023

[20] S. Fuchs and J. Biela, "Impact of the Prediction Error on the Performance of Model Predictive Controllers with Long Prediction Horizons for Modular Multilevel Converters - Linear vs. Nonlinear System Models," *2018 20th European Conference on Power Electronics and Applications (EPE'18 ECCE Europe),* 2018, pp. P.1-P.9.

[21] S. Fuchs, M. Jeong and J. Biela, "Long Horizon, Quadratic Programming Based Model Predictive Control (MPC) for Grid Connected Modular Multilevel Converters (MMC)," *IECON 2019 - 45th Annual Conference of the IEEE Industrial Electronics Society,* 2019, pp. 1805-1812

[22] M. Aguirre, S. Kouro, C. A. Rojas, J. Rodriguez and J. I. Leon, "Switching Frequency Regulation for FCS-MPC Based on a Period Control Approach," *IEEE Transactions on Industrial Electronics*, vol. 65, no. 7, pp. 5764-5773, July 2018

[23] P. Karamanakos, E. Liegmann, T. Geyer and R. Kennel, "Model Predictive Control of Power Electronic Systems: Methods, Results, and Challenges," *IEEE Open Journal of Industry Applications*, vol. 1, pp. 95-114, 2020

[24] X. Chen, J. Liu, S. Song, S. Ouyang, H. Wu and Y. Yang, "Modified Increased-Level Model Predictive Control Methods With Reduced Computation Load for Modular Multilevel Converter," *IEEE Transactions on Power Electronics*, vol. 34, no. 8, pp. 7310-7325, Aug. 2019